Scientific Research Publishing

Open Journal of Inorganic Chemistry, 2023, 13, 25-42
https://www.scirp.org/journal/ojic
ISSN Online: 2161-7414
ISSN Print: 2161-7406

Fixed-Bed Column Adsorption Modeling of MnO_4^- Ions from Acidic Aqueous Solutions on Activated Carbons Prepared with the Biomass

Charly Mve Mfoumou[1,2*], Francis Ngoye[1], Pradel Tonda-Mikiela[1,2], Mbouiti Lionel Berthy[1,2], Bouassa Mougnala Spenseur[1,2], Guy Raymond Feuya Tchouya[1,2]

[1]Laboratoire de Chimie des Milieux et des Matériaux Inorganiques (LC2MI), URCHI, Université des Sciences et Techniques de Masuku (USTM), Franceville, Gabon
[2]Département de Chimie, Faculté des Sciences, Université des Sciences et Techniques de Masuku (USTM), Franceville, Gabon
Email: *charly.mvemfoumou@univ-masuku.org, *mvefoumou@gmail.com

How to cite this paper: Mfoumou, C.M., Ngoye, F., Tonda-Mikiela, P., Berthy, M.L., Spenseur, B.M. and Tchouya, G.R.F. (2023) Fixed-Bed Column Adsorption Modeling of MnO_4^- Ions from Acidic Aqueous Solutions on Activated Carbons Prepared with the Biomass. *Open Journal of Inorganic Chemistry*, **13**, 25-42.
https://doi.org/10.4236/ojic.2023.132002

Received: January 30, 2023
Accepted: April 27, 2023
Published: April 30, 2023

Abstract

Activated carbons calcined at 400˚C and 600˚C (AC-400 and AC-600), prepared using palm nuts, collected in the town of Franceville in Gabon, were used to study the dynamic adsorption of MnO_4^- ions in acidic media on fixed bed column and on the kinetic modeling of experimental data of breakthrough curves of MnO_4^- ions obtained. Results on the adsorption of MnO_4^- ions in fixed-bed dynamics obtained on AC-400 and AC-600 adsorbents beds indicated that the AC-400 bed appears to be the most efficient in removing MnO_4^- ions in acidic media. Indeed, the adsorbed amounts, the adsorbed capacities at saturation and the elimination percentage of MnO_4^- ions obtained with AC-400 (31.24 mg; 52.06 $mg \cdot g^{-1}$ and 41.65% respectively) were higher compared to those obtained with AC-600 (9.87 mg; 16.45 $mg \cdot g^{-1}$ and 17.79% respectively). The breakthrough curves kinetic modeling revealed that the Thomas model and the pseudo-first-order kinetic model were the most suitable models to describe the adsorption of MnO_4^- ions on adsorbents studied in our experimental conditions. The results of the intraparticle diffusion model showed that intraparticle diffusion was involved in the adsorption mechanism of MnO_4^- ions on investigated adsorbents and was not the limiting step and the only process controlling MnO_4^- ions adsorption. In contrast to AC-400, the intraparticle diffusion on AC-600 bed plays an important role in the adsorption mechanism of MnO_4^- ions.

Keywords

Acidic Media, MnO_4^-, Biomass, Activated Carbon, Dynamic Adsorption, Kinetics Models

1. Introduction

In order to diversify its economy, Gabon created the company "Olam Palm Gabon" with the Singaporean group Olam for the development of the palm oil sector with the objective of being the first industrial producer of palm oil in the African continent [1]. Today, OLAM Palm Gabon owns nearly 300,000 hectares of forest and over 4322 hectares of palm trees plantations [1]. This large scale oil production generates important amounts of waste, including palm nuts shells, which cause visual and environmental pollution. It is then important to find solutions for the reduction of this type of pollution. One solution is the use of palm nut shells as raw material in the preparation of solid adsorbents of activated carbon type.

Indeed, the raw materials used in the preparation of activated carbons can be from animal (animal bones), minerals (coal) and vegetables (plants, bark etc.) [2] [3] [4] [5]. A particular interest is made for materials of plant origin such as lignocellulosic biomass of agricultural waste type. In fact, these latter are: renewable, inexpensive and easily available source [2]. Palm nut shells, due to their carbon, lignin and hemicellulose content and their capacity to produce microporous activated carbons, are of particular interest in the production of this type of adsorbent [3]. These porous solid materials are capable of trapping or eliminating at their surface, or in their porous structures, organic or mineral pollutants in the form of ionic toxic species ($Cr_2O_7^{2-}$; MnO_4^- …) in aqueous media [6] [7]. For example, in Gabon, the intensity of mining activities in the extraction of manganese (Mn), in Moanda and Franceville, in the Haut Ogooué province, has resulted in higher manganese concentrations in the surrounding soils and environment [8]. Mn is one of the inorganic pollutants sensitive to redox reactions and can form anionic species of the MnO_4^- type under certain media conditions [7]. These species can also be generated following disinfection processes of potable water and in the elimination of organic substances from wastewater through oxidation processes [9] [10]. MnO_4^- ions can cause irritation to the skin, eyes, destruction of the liver and kidneys in case of splashing or oral ingestion [10]. Considering the toxic nature of MnO_4^- ions, the World Health Organization (WHO) recommends a limit of 0.5 $mg{\cdot}L^{-1}$ of MnO_4^- ions in wastewater [11]. Many studies have investigated the adsorption or removal of MnO_4^- ions on activated carbons in aqueous solution, by evaluating the effect of experimental conditions (pH and concentration of initial solution, adsorbent mass, particle size, etc.) in order to determine the bed efficiency and adsorption capacities of activated carbons [12] [13] [14]. It appears that the experimental condi-

tions have a strong influence on the efficiency of the adsorbent bed to trap MnO_4^- type pollutants. So, in acidic media, removal of MnO_4^- ions seems to be more efficient on the activated carbons.

Thus, the aims of this study were to prepare the activated carbons from the palm nut shells, collected in the city of Franceville in Gabon and to carry out the adsorption of MnO_4^- ions in dynamic conditions at fixed bed in acidic media. The application of Thomas, Adams-Bohart and pseudo first and pseudo second order kinetic models on experimental data of MnO_4^- ions adsorption has also been realized.

2. Experimental

2.1. MnO_4^- Ions Solution Preparation

1 g·L^{-1} of MnO_4^- ions solution were prepared by dissolving in distilled water 1 g of extra-pure crystallized potassium permanganate ($KMnO_4$) from Scharlab SL, in a flask of 1 L. The solution was stirred during 15 minutes. Then by dissolution, a 50 mg·L^{-1} solution was prepared. The 50 mg·L^{-1} solution was used to study the adsorption of MnO_4^- ions on activated carbons.

2.2. Preparation Method of Activated Carbons

Activated carbons (AC) were prepared using the palm nut shells collected in the city of Franceville in the Haut Ogooué region of Gabon. All procedure of preparation of AC was reported in a recent study [13].

However after impregnation at a zinc chloride solution to 1 M (1:1 ratio) and drying, the solids were activated at 400˚C and 600˚C for 1 h and 30 minutes (min) using a rise in temperature of 5˚C·min^{-1}. The activated carbons obtained were cooled, rinsed with 0.1 M HCl and washed with distilled water until the pH of the residual water being equal to 6.5. Then dried in the oven for 48 h at 100˚C and sieved to have granular activated carbons with particle sizes $0.04 < x < 0.1$ mm (sieves used: TAMISAR (Norm: AFNOR_NF-X11-501).

Activated carbons obtained at 400˚C and 600˚C will be designated AC-400 and AC-600 respectively.

2.3. Adsorbents Characterizations

Data on the surface areas and pore volumes were carried out using a Micromeritics TRISTAR 3000 instrument following T. Belin method [15]. About 100 mg of activated carbon sample was pretreated during 1 h at 90˚C, and 10 h at 350˚C successively. Physisorption isotherms of nitrogen (N_2) were carried out at −196˚C. The specific surface areas of samples were evaluated by means of the Brunauer, Emmett and Teller (BET) theory [16]. Microporous and mesoporous volumes were determined by t-plot method of De Boer and Dubinin-Radushkevich equations respectively [17] [18] [19].

The pH at the point of zero charge (pH_{PZC}) of activated carbons was obtained

based on the acid-base titration method described by Amola [20] and reproduced in in a recent study [13]. The pH_{PZC} of activated carbons are given by the point of intersection between the experimental curves and the theoretical curves of pHf = f(pHi).

Assessments of surface function groups of activated carbons were performed using the Boehm method, with little modifications [13] [21]. The number of equivalents ($m_{eq}\cdot g^{-1}$) or concentrations ($mmol\cdot g^{-1}$) of acid or basic groups were calculated using the following equation:

$$n\left(\text{mmol}\cdot\text{g}^{-1}\right)=\frac{C\times\left(V_{eq.b}-V_{eq.s}\right)\times 1000}{m_{AC}}$$

C is the concentration of NaOH or HCl ($mol\cdot L^{-1}$); $V_{eq.b}$ and $V_{eq.s}$ are the equivalent volumes of the blank and sample (L) respectively; m_{AC} is the mass of activated carbon (g) and 1000 is the conversion factor in mmol.

2.4. Fixed-Bed Column Adsorption Experiments

Experiments of the adsorption of MnO_4^- ions on activated carbons were carried out at room temperature (25˚C) in a pyrex brand glass column of a length of 50 cm and diameter 2.4 cm, in dynamic mode on fixed-bed column. The protocol and scheme of the experimental set-up of the adsorption process were reported in our previous study [13].

Adsorption experiments were carried out with flow rates of 3 $mL\cdot min^{-1}$, on the activated carbon beds composed grains with particle sizes $0.04 < x < 0.1$ mm. The initial concentration (C_0) and pH solutions of MnO_4^- ions used were of 50 $mg\cdot L^{-1}$ and 3.5 respectively. The experiments were stopped when the beds were saturated, *i.e.* when the residual concentrations (C) were equal to the concentrations at the inlet of the column (C_0) ($C/C_0 = 1$). An area (A) in minutes is obtained by integration according to the trapeze method [13] [22] [23]:

$$A(\text{min})=\sum_n \frac{\left(1-\frac{C_{t_n}}{C_0}\right)+\left(1-\frac{C_{t_{n+1}}}{C_0}\right)}{2}\times\left(t_{n+1}-t_n\right)$$

C_0 and C are the inlet and outlet concentrations ($mg\cdot L^{-1}$) at times t_n and t_{n+1} respectively.

Adsorbed amounts of MnO_4^- ions (q_{ads}) and saturation adsorption capacities (Q_{sat}) are calculated by the following relations:

$$q_{ads}\left(\text{mg}\right)=D\cdot C_0\cdot A$$

$$Q_{sat}\left(\text{mg}\cdot\text{g}^{-1}\right)=\frac{D\cdot C_0\cdot A}{m_{AC}}$$

D, C_0, A and m_{AC} correspond to the flow rate ($mL\cdot min^{-1}$), the concentration at the inlet of the column ($mg\cdot L^{-1}$), the area surface corresponding to the adsorbed amount of MnO_4^- (min) and the activated carbon mass used (g) respectively.

Removal percentages (E) of manganese ions (MnO_4^-) on activated carbons are

given by the relation:

$$E(\%) = \frac{A}{t_{sat}} \times 100$$

t_{sat} is the saturation time (min).

2.5. Fixed-Bed Column Adsorption Mathematical Models

Thomas and Adams-Bohart models are the most widely used mathematical models to describe the dynamic behavior of metallic pollutants in adsorption on fixed bed columns. These models were applied to experimental data of breakthrough curves obtained in our study. The pseudo-first and pseudo-second order kinetic models, as well as the intraparticle diffusion model were also applied.

2.5.1. Thomas and Adams-Bohart Models

The Thomas model (1944) repeated by Saadi [24] assumes that external and internal diffusion limitations are not present during the fixed-bed column adsorption process, that the driving force follows the Langmuir isotherm and second-order reversible reaction kinetics considering that the adsorption of pollutant is not limited by the chemical reaction, but is controlled by mass transfer at the interface.

The mathematical expression for this model is as follows:

$$\frac{C}{C_0} = \frac{1}{1 + \exp\left[\frac{k_{Th} \cdot q_e \cdot m_{AC}}{D} - k_{Th} \cdot C_0 \cdot t\right]}$$

The linear form of this equation is:

$$\ln\left(\frac{C}{C_0} - 1\right) = \frac{k_{Th} \cdot q_e \cdot m_{AC}}{D} - k_{Th} \cdot C_0 \cdot t$$

where k_{Th} (mL·min^{-1}·mg^{-1}) is the Thomas model constant, q_e (mg·g^{-1}) is the theoretical adsorption capacity, m_{AC} is activated carbon mass (g), D is flow rate (mL·min^{-1}), C_0 is initial solution concentration (mg·L^{-1}), and C is residual (or equilibrium) concentrations in outlet column (mg·L^{-1}).

The assumption on which based the Adams-Bohart model (1920) [24] is that the rate of adsorption is proportional to both the concentration of the adsorbing species and the residual capacity of the adsorbent and is only used for the description of the initial part of the breakthrough curve. The mathematic expression of this model is:

$$\frac{C}{C_0} = \exp\left(k_{AB} \cdot C_0 \cdot t - k_{AB} \cdot N_0 \cdot \frac{h}{U_0}\right)$$

The linear form of this expression is:

$$\ln\left(\frac{C}{C_0}\right) = k_{AB} \cdot C_0 \cdot t - k_{AB} \cdot N_0 \cdot \frac{z}{U_0}$$

where k_{AB} is rate constant of Adams-Bohart model (L·min^{-1}·mg^{-1}), z (cm) is the

bed depth, N_0 is maximum adsorption capacity per unit volume of adsorbent column (mg·L^{-1}), and U_0 is the linear velocity of influent solution (cm·min^{-1}).

2.5.2. Pseudo First and Pseudo Second Order and Intraparticle Kinetic Models

To evaluate the adsorption mechanism and the mode of transfer of solutes from the liquid phase to the solid phase, the pseudo first order kinetic models developed by Lagergren [25], the pseudo second order developed by Blanchard and linearized by Ho [26] [27] and the Weber and Morris model [28] were applied to experimental data of MnO_4^- breakthrough curves.

The expression of the rate law of a pseudo first order reaction is [29]:

$$\frac{\mathrm{d}q_t}{\mathrm{d}t} = k\left(q_e - q_t\right)$$

And by integration between $t = 0$ and t, and at $q_t = 0$ and q_t. We then obtain the following linear form:

$$\log\left(q_e - q_t\right) = \log q_e - \frac{k_1}{2.3}\cdot t$$

where q_t and q_e correspond to maximum adsorption capacities at time t and equilibrium (mg·g^{-1}) respectively, and k_1 the adsorption rate constant of the pseudo-first order kinetic model (min^{-1}).

The pseudo-second order model is given by the following relation [28]:

$$\frac{\mathrm{d}q}{\mathrm{d}t} = k_2\left(q_e - q_t\right)^2$$

And after integration between $t = 0$ and t, then when $q_t = 0$ and q_t, we obtain the following linear form:

$$\frac{t}{q} = \frac{1}{k_2 \cdot q_e^2} + \frac{1}{q_e}\cdot t$$

where q_t and q_e correspond to maximum adsorption capacities at time t and equilibrium (mg·g^{-1}) respectively, and k_2 the adsorption rate constant of the pseudo-first order kinetic model (g·mg^{-1}·min^{-1}).

According to Webber and Morris [29], the kinetic expression of intraparticle diffusion is described by:

$$q_t = k_d \cdot t^{1/2} + C_d$$

k_d is the intraparticle diffusion rate constant (mg·g^{-1}·min$^{1/2}$) and C_d, intercept of the curve. C_d gives an indication of the thickness of the boundary layer and/or adhesion to the surface [13] [29].

3. Results and Discussion

3.1. Characterizations of Prepared AC

Textural and chemical characteristics of prepared activated carbons (AC) were evaluated. The textural study was performed by N_2 physisorption. To evaluate the chemical properties, the pH at zero charge point (pH_{PZC}) of ACs were deter-

mined and the quantifications of the surface function groups were performed on each adsorbent.

Figure 1 shows the N_2 adsorption/desorption isotherms obtained on prepared activated carbons AC-600 and AC-400. These isotherms show the same profile. A rapid adsorption was observed in the range of pressure ratio (P/P_0) between 0.0 - 0.3, followed by a plateau for P/P_0 between 0.3 - 0.9.

Based on the IUPAC classification [30], the isotherms obtained are of type I. these isotherms are characteristic of microporous materials. Also, they show hysteresis loops of type H4, indicating slit shaped pores.

Table 1 presents the specific surface areas (S_{BET}) and total pore volumes of studied adsorbents after exploitation of N_2 physisorption isotherms. The AC-400 adsorbent shows a S_{BET} (182.4 $mg^2 \cdot g^{-1}$), a total pore volume (0.078 $cm^3 \cdot g^{-1}$) and a microporous volume (0.073 $cm^3 \cdot g^{-1}$) higher than those obtained with the prepared activated carbon AC-600 (116.2 $mg^2 \cdot g^{-1}$, 0.049 $cm^3 \cdot g^{-1}$ and 0.043 $cm^3 \cdot g^{-1}$ respectively). It seems that in our experimental conditions, an increase of the calcination temperature in the preparation of activated carbons ($T_{calcination} > 400^\circ C$), causes a loss of specific surface and pore volumes.

The mesoporous volumes obtained, for all prepared activated carbons (AC-600 and AC-400: 0.002 and 0.001 $cm^3 \cdot g^{-1}$ respectively), are negligible compared to those of microporous (Table 1). Then, the prepared activated carbons present porous structures mainly consisting of microporous.

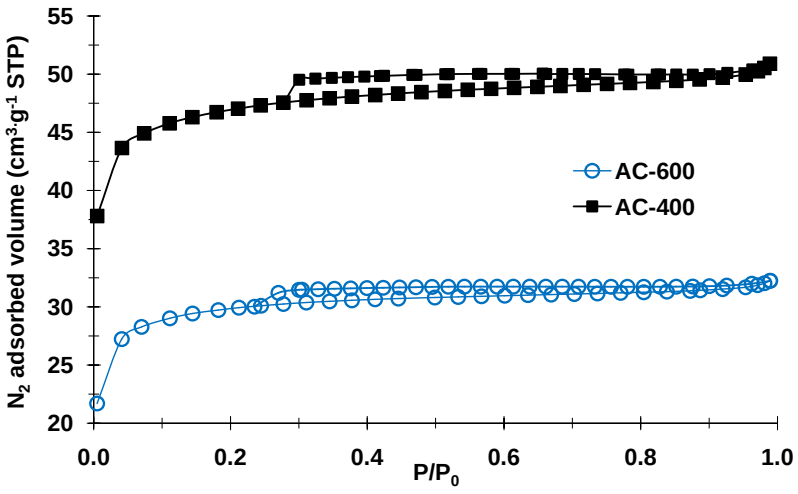

Figure 1. Isotherms of N_2 physisorption obtained on prepared activated carbons AC-600 and AC-400.

Table 1. Structural and chemical properties obtained on AC-600 and AC-400 adsorbents.

Adsorbents	S_{BET} ($m^2 \cdot g^{-1}$)	$V_{micro.}$ ($cm^3 \cdot g^{-1}$)	$V_{meso.}$ ($cm^3 \cdot g^{-1}$)	$V_{total\ pore}$ ($cm^3 \cdot g^{-1}$)	pH_{PZC}	Basic functions ($mmol \cdot g^{-1}$)	Acidic functions ($mmol \cdot g^{-1}$)			
							Total	Carboxyl	Lactone	Phenol
AC-600	116.2	0.046	0.002	0.049	6.7	0.55	3.21	0.20	0.63	2.38
AC-400	182.4	0.073	0.001	0.078	4.9	0.25	3.45	0.35	0.75	2.35

Figure 2 shows the curves obtained in the determination of the pH at zero charge point (pH_{PZC}) of AC-600 and AC-400 adsorbents. Results reveal that the surface of AC-400 adsorbent is more acidic than that of AC-600 activated carbon. Indeed, the pH_{PZC} obtained on AC-400 (4.9) is higher than that of AC-600 (6.7). The accessible surfaces or adsorption sites on AC-400 could interact more strongly with the anionic species MnO_4^- due to its acidic character. Chemical type reactions (irreversible) can take place at the surface of this adsorbent during the adsorption of MnO_4^- ions.

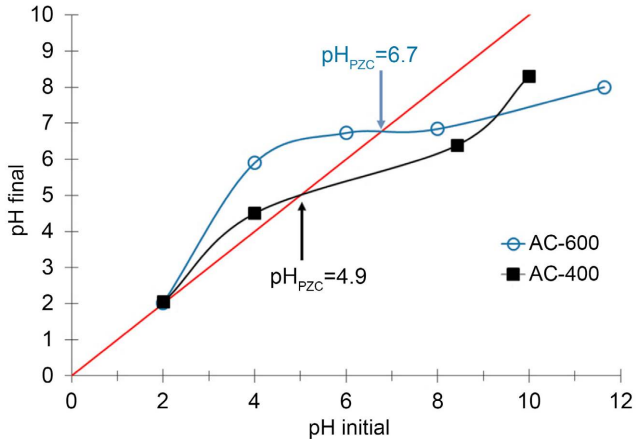

Figure 2. Curves obtained for the determination of pH_{PZC} of AC-600 and AC-400 adsorbents, using the acid-base titration method [20].

In addition, these results indicate that the surfaces of activated carbons is positively charged when the pH of the solution (pH_{sol}) is less than their pH_{PZC} and is negatively charged when the pH is above their pH_{PZC} [13]. Thus, interactions between the surface of activated carbons and MnO_4^- ions will be more important at $pH_{sol} < pH_{PZC}$ for each adsorbent.

Results of the quantification of concentrations of surface functions of prepared activated carbons are reported in Table 1. Based on these results, the amounts of acidic function groups obtained on AC-600 and AC-400 are close (3.21 and 3.45 $mmol \cdot g^{-1}$ respectively). Regardless of the prepared activated carbons, phenol functional groups are in majority on the surface of adsorbents (Table 1). Lactone and carboxylic acid functional groups appear to be in minority. Compared to amounts of acidic function groups, the amounts of basic function groups obtained on AC-600 and AC-400 (0.55 and 0.25 $mmol \cdot g^{-1}$ respectively) are very low.

3.2. Fixed-Bed Column Dynamic Adsorption

Figure 3 shows the breakthrough curves of MnO_4^- ions obtained on AC-400 and AC-600 adsorbents at 25˚C. These breakthrough curves show a multi-step adsorption mode (3 zones) in the form of staircase, with different adsorption kinetics and diffusions according to form of slopes of each adsorption domain. These curve profiles are similar to those obtained in a previously study [13]. On the other hand, this phenomenon (multi-step adsorption mode) appears more

visible on the AC-400 adsorbent with slow adsorption and/or diffusion rates between the grains or on the surface of the solid. Also, the interactions between MnO_4^- ions and the AC structure seem to be stronger on the AC-400 adsorbent based on the slopes of the different adsorption domains of the breakthrough curve of this porous solid [13].

It seems that on this adsorbent we have a better distribution of adsorption sites favorable to the removal of MnO_4^- ions. This appears to be related to adsorption surfaces (adsorption sites) that are available on AC-400. Indeed, the surface area and pore volumes obtained on AC-400 are higher than those calculated on AC-600 (**Table 1**).

In addition in our operating conditions, the AC-400 bed appears to be the most efficient in removing MnO_4^- ions (**Figure 3**). The breakthrough and saturation times obtained on AC-400 (25 and 500 min respectively) are higher than those obtained on AC-600 (3 and 370 min respectively). The effect of accessible surfaces on AC-400 seems to be verified.

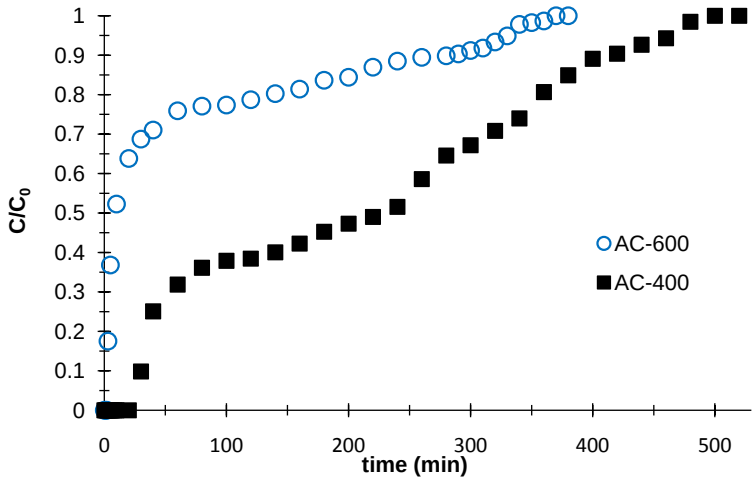

Figure 3. Breakthrough curves of MnO_4^- ions obtained at 25˚C on beds of AC-400 and AC-600 adsorbents composed of particle size $0.01 < x < 0.04$ (H = 0.5 cm, D = 3 mL·min^{-1}, C_0 = 50 mg·L^{-1} and pH = 3.5).

Table 2 summarizes, after exploitation of breakthrough curves data, the contact time (t_c) of the flow rate of MnO_4^- solution and the activated carbons bed, the breakthrough and saturation times (t_b and t_{sat} respectively), the adsorbed amounts of MnO_4^- ions (q_{ads}) and saturation adsorption capacities (Q_{sat}), and the removal percentages of MnO_4^- ions of each adsorbent.

These results confirm the predictions of breakthrough curves. Indeed, the adsorbed amounts, the adsorbed capacities at saturation and the elimination percentage of MnO_4^- ions in acidic media obtained on the bed composed of AC-400 (31.24 mg; 52.06 mg·g^{-1} and 41.65% respectively) are higher compared to those obtained with the AC-600 activated carbon (**Table 2**).

Since adsorption is a surface phenomenon, the more the surface areas are accessible, the more the adsorption capacities of MnO_4^- ions in aqueous solution

[13] [31] and, in consequence, the functional groups on the surface of activated carbons will be important and more accessible. These surface function groups characterized before, (carboxylic acid, lactone and phenol) can produce, by protonation in acidic aqueous solution, new adsorption sites favorable to MnO_4^- / activated carbon structure interactions or to new adsorption sites [31], which would increase the adsorption capacities of MnO_4^- ions on AC beds in our experimental conditions.

Based on these results, the prepared activated carbon can be used in fixed bed dynamic adsorption processes for the removal of MnO_4^- ions from acidic aqueous solution, in particular the AC-400 adsorbent whose bed shows a better efficiency.

Table 2. Results of the adsorption of MnO_4^- ions in fixed-bed dynamics obtained at 25˚C on beds of AC-400 and AC-600 adsorbents composed of particle size $0.01 < x < 0.04$ ($H = 0.5$ cm, $D = 3$ mL·min^{-1}, $C_0 = 50$ mg·L^{-1} and pH = 3.5).

Adsorbents	t_c (s)	t_b (min)	t_{sat} (min)	q_{ads} (mg)	Q_{sat} (mg·g^{-1})	E (%)
AC-400	45	25	500	31.24	52.06	41.65
AC-600		3	370	9.87	16.45	17.79

3.3. Breakthrough Curves Kinetic Modeling

3.3.1. Thomas and Adams-Bohart Models

In order to understand the phenomena and/or describe the dynamic behavior of MnO_4^- ions removal in adsorption on fixed bed columns, the Thomas model [23] and Adams-Bohart model [32] were applied to the data of breakthrough curves obtained on activated carbons studied.

Figure 4 and **Figure 5** show the linear plots obtained after application of Thomas and Adams-Bohart linear models on experimental data of breakthrough curves of MnO_4^- ions dynamic adsorption on AC-600 and AC-400 adsorbents.

Based on the results of both linear models, the Thomas model is the model that is in good agreement with the experimental points (**Figure 4** and **Figure 5**). Indeed, the linear regression coefficients (R^2) obtained with the Thomas model (**Table 3**) are close to the unit, in particular on AC-600 activated carbon, where the $R^2 = 0.985$. This is not the case for the Adams-Bohart linear model.

In addition, the maximum adsorption capacities calculated following the Thomas model on AC-400 and AC-600 (48.988 and 20.063 mg·g^{-1} respectively) are close to experimental values (52.057 and 16.454 mg·g^{-1}). In contrast, the Adams-Bohart model predicts high adsorbed quantities at saturation (N_0) on AC-600 and AC-400 (**Table 3**).

The Thomas model can be used to describe, in our experimental conditions, the mechanisms (diffusion, mass transfer, kinetics…), to characterize the behavior of MnO_4^- ions during the removal on AC-400 and AC-600 in dynamic adsorption on fixed bed columns (reaction on the surface in particular) and to predict breakthrough curves.

Thus, according to the Thomas model, the external and internal diffusion li-

mitations are not present in our dynamic adsorption experiments on fixed bed column of MnO_4^- ions and so, the driving force follows the Langmuir isotherm and reversible reaction kinetics, showing that, MnO_4^- ions are not limited by the chemical reaction, but are controlled by the mass transfer at the interface.

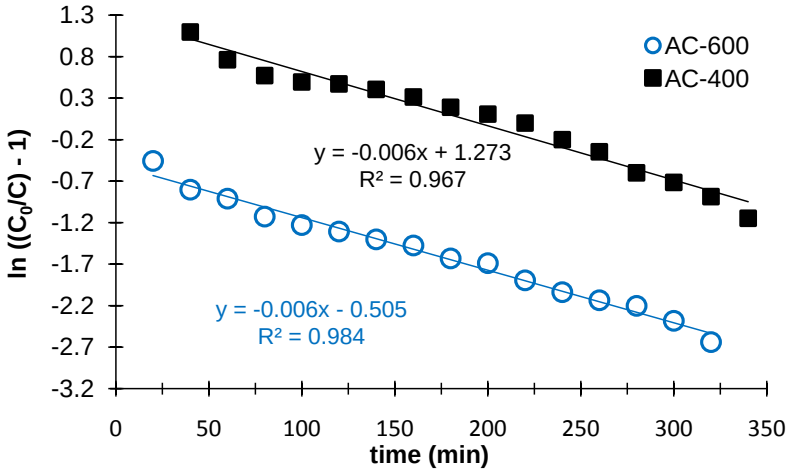

Figure 4. Linear plots of Thomas model on experimental data (breakthrough curves) of MnO_4^- ions adsorption on AC-600 and AC-400 adsorbents.

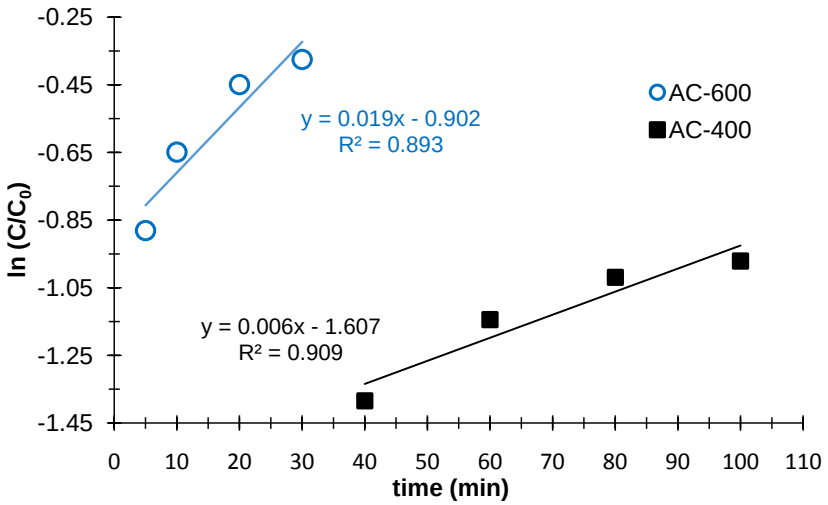

Figure 5. Linear plots of Adams-Bohart model on experimental data (breakthrough curves) of MnO_4^- ions adsorption on AC-600 and AC-400 adsorbents.

Table 3. Experimental Q_e and parameters of Thomas and Adams-Bohart models of the dynamic adsorption on fixed-bed column of MnO_4^- ions on AC-600 and AC-400 adsorbents.

		Thomas model			Adams-Bohart model			
Adsorbents	$Q_{e,exp}$ (mg·g^{-1})	$q_{e,cal}$ (mg·g^{-1})	k_{Th} (mL·mg^{-1}·min^{-1})	R^2	U_0 (cm·min^{-1})	N_0 (mg·L^{-1})	k_{AB} (mL·mg^{-1}·min^{-1})	R^2
AC-600	16.45	20.06	0.126	0.985	0.667	116.12	2.591	0.893
AC-400	52.06	48.99	0.130	0.967		72.86	7.353	0.909

On the other hand, the rate constants of Thomas model (k_{Th}) calculated for AC-600 and AC-400 (0.126 and 0.130 $mL \cdot mg^{-1} \cdot min^{-1}$ respectively) are quite similar. It seems that, whatever the adsorbent, in our experimental conditions, the adsorption rate (or adsorption kinetics) of MnO_4^- ions on prepared activated carbons is not different.

3.3.2. Kinetic Models of Pseudo-First and Pseudo-Second Order

To identify kinetics that control the adsorption mechanism of MnO_4^- ions on studied activated carbons in our experimental conditions, pseudo-first and pseudo-second order kinetic models were applied to experimental data from breakthrough curves of MnO_4^- ions.

Figure 6 and Figure 7 show the linear plots obtained after application of the linear equation of these kinetic models on experimental data of breakthrough curves.

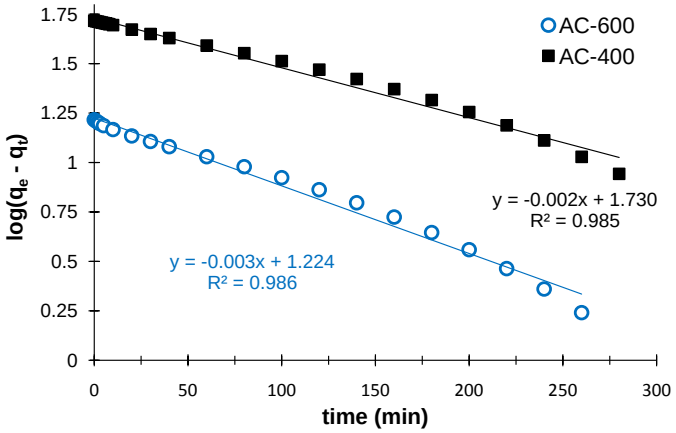

Figure 6. Pseudo-first-order kinetic model applied to experimental data (breakthrough curves) of MnO_4^- ions adsorption on AC-600 and AC-400 adsorbents.

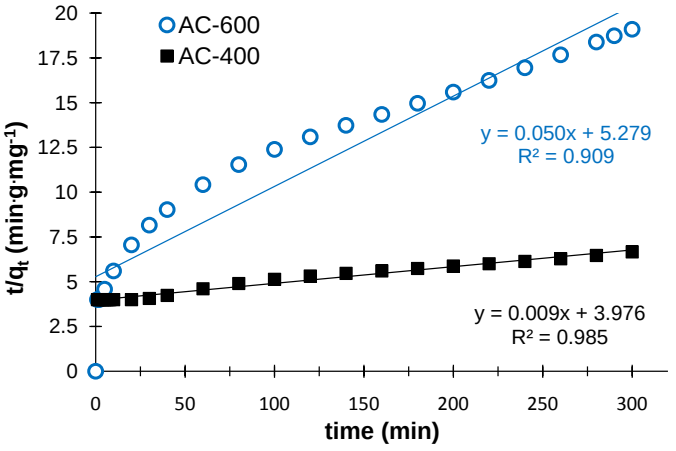

Figure 7. Pseudo-second-order kinetic model applied to experimental data (breakthrough curves) of MnO_4^- ions adsorption on AC-600 and AC-400 adsorbents.

Based on linearization results, the pseudo first order kinetic model is in good agreement with the experimental points. Also, error percentages between the calculated and experimental equilibrium capacities ($q_{e.cal}$ and $Q_{e,exp.}$ respectively) obtained on AC-600 and AC-400 are about 3 and 2% (Table 4). Indeed, the $q_{e,cal.}$ obtained on AC-600 and AC-400 (16.752 and 53.777 $mg{\cdot}g^{-1}$ respectively) are close to the $Q_{e,exp.}$ (16.454 and 52.057 $mg{\cdot}g^{-1}$ respectively), contrary to results obtained for pseudo-second-order model (Table 4). Moreover, the R^2 values obtained for AC-600 and AC-400 (0.986 and 0.985 respectively) are close to 1. These results are very different from those obtained by Nasser A. *et al.* where MnO_4^- ions were adsorbed on porous solids in static mode [33].

Table 4. Experimental Q_e and parameters values of pseudo-first and pseudo-second order kinetic models of the dynamic adsorption on fixed-bed column of MnO_4^- ions on AC-600 and AC-400 adsorbents.

Adsorbents		Pseudo-first order			Pseudo-second order		
	$Q_{e,exp.}$ ($mg{\cdot}g^{-1}$)	$q_{e,cal.}$ ($mg{\cdot}g^{-1}$)	k_1 ($min^{-1}{\cdot}10^{-4}$)	R^2	$q_{e,cal.}$ ($mg{\cdot}g^{-1}$)	k_2 ($g{\cdot}mg^{-1}{\cdot}min^{-1}{\cdot}10^{-4}$)	R^2
AC-600	16.45	16.75	58	0.986	19.84	4.81	0.909
AC-400	52.06	53.78	78	0.985	107.53	0.22	0.985

Thus, results obtained according to the Thomas model seem to be verified. Rate constants (k_1) obtained on AC-600 and AC-400 (0.0058 and 0.0078 min^{-1}) are almost similar and based on the pseudo first order kinetics model, the reactions at the surface between MnO_4^- ions and adsorption sites are more reversible (physisorption).

On the other hand, chemical reactions, in our experimental conditions, are not excluded on the surface of activated carbons studied. According to the results of the pseudo-second order kinetic model, the adsorption of MnO_4^- ions, in particular on the AC-400 bed, follows this model. Indeed, the experimental points are in agreement with the model (Figure 7) and the R^2 value obtained (0.985) is similar to that obtained with the pseudo first order kinetic model (Table 4). It appears thus that on the bed of activated carbons studied, chemical reactions (chemisorption) between MnO_4^- ions and the surface of the adsorbents exist also in our experimental conditions.

However, the pseudo-first order kinetic model is the model that best describes the adsorption of MnO_4^- ions from acidic aqueous solutions in fixed bed column dynamics on activated carbons studied.

3.3.3. Intraparticle Kinetic Model

The intraparticle kinetics model was applied to the experimental data of MnO_4^- ions breakthrough curves to evaluate the diffusion phenomenon that controls the adsorption of MnO_4^- ions on activated carbon beds studied (Figure 8).

Based on the linear plot results obtained, the plots do not intersect through the origin ($C_d \neq 0$). This implies that intraparticle diffusion is involved in the adsorption mechanism of MnO_4^- ions on investigated adsorbents and is not the

limiting step and the only process controlling MnO_4^- ions adsorption in our experimental conditions [13] [34].

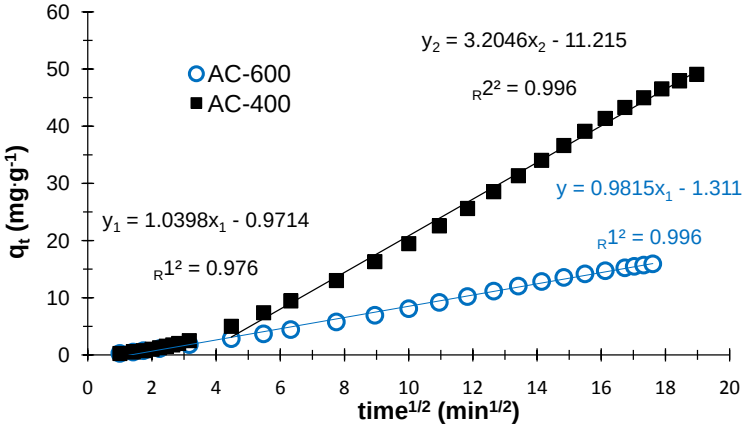

Figure 8. Intraparticle kinetic model applied to experimental data from the study of the adsorption of MnO_4^- ions on AC-600 and AC-400 adsorbents.

In contrast to AC-400, with the AC-600 adsorbent, we obtain a slope with a coefficient of linear regression R^2 = 0.997 close to 1. This result reveals that intraparticle diffusion on the AC-600 bed plays an important role in the adsorption mechanism of MnO_4^- ions. On the other hand, the two (2) linear domains obtained on AC-400 show that on this adsorbent, we have a multi-stage adsorption as indicated on the breakthrough curves. Similar results were observed in a recent study [13].

The value of the intraparticle diffusion rate constant (k_{d_1}) obtained on AC-400 (1.039 mg·min$^{-1/2}$·g^{-1}) is comparable to that obtained on AC-600 (0.982 mg·min$^{-1/2}$·g^{-1}). It seems that in this first linear (or adsorption) domain of AC-400, the diffusion rate of MnO_4^- ions in the porosity (or between the pores) is the same as on AC-600. The comparable microporous structures of studied adsorbents seem to be related to this result.

The intercept curve C_d (**Table 5**) represents the thickness of the boundary layer and greater the C_d value, greater the contribution to surface adhesion in the speed limit step [31]. Comparing the value obtained on AC-400 from the second linear domain with that of the adsorbent AC-600, it appears that the adherence of MnO_4^- ions to the surface of AC-400 is about 11 times higher. It seems that the acidic character of AC-400 whose pH_{PZC} = 4.9 based on the results in **Table 1**, is related to this result. The MnO_4^- ions interact more strongly with the structure of the prepared activated carbon AC-400 in acidic media. The hypothesis of chemisorption between the MnO_4^- ions and the structure of this adsorbent (adsorption sites) appears more obvious.

However, the C_d values obtained on the activated carbons studied are relatively high, this confirm the fact that intraparticle diffusion is not the limiting step and rather that surface adsorption plays a predominant role in the adsorption of MnO_4^- ions on activated carbons studied in acidic media.

Table 5. Parameters of intraparticle kinetic model of the dynamic adsorption on fixed-bed column of MnO_4^- ions on AC-600 and AC-400 adsorbents.

Adsorbents	Region 1			Region 2		
	k_{d_1} ($mg \cdot min^{-1/2} \cdot g^{-1}$)	C_{d_1}	R_1^2	k_{d_2} ($mg \cdot min^{-1/2} \cdot g^{-1}$)	C_{d_2}	R_2^2
AC-600	0.982	1.311	0.997	-	-	-
AC-400	1.039	0.971	0.976	3.205	11.215	0.996

4. Conclusions

The objective of the work was to investigate the dynamic fixed-bed adsorption of MnO_4^- ions on activated carbons prepared from palm nuts and activated at 400 and 600˚C (AC-400 and AC-600 respectively). Prepared adsorbents were characterized texturally and chemically.

Textural characterizations by nitrogen (N_2) physisorption showed materials with mainly microporous structures. However, it appears that in our experimental conditions, an increase of the calcination temperature in the preparation of activated carbons ($T_{calcination} > 400$˚C), causes to a loss of specific surface and pore volumes.

Results of experiments on the adsorption of MnO_4^- ions in fixed-bed dynamics obtained on beds of AC-400 and AC-600 adsorbents indicate that the AC-400 bed appears to be the most efficient in removing MnO_4^- ions in acidic media. The adsorbed amounts, the adsorbed capacities at saturation and the elimination percentage of MnO_4^- ions obtained on the bed containing AC-400 (31.24 mg; 52.06 $mg \cdot g^{-1}$ and 41.65% respectively) are higher compared to those obtained on the AC-600 activated carbons (9.87 mg; 16.45 $mg \cdot g^{-1}$ and 17.79% respectively).

Study of the breakthrough curves kinetic modeling reveals that the Thomas model and the pseudo-first-order kinetic model are the most suitable models to describe the adsorption of MnO_4^- ions on the adsorbents studied in our experimental conditions. The results of the intraparticle diffusion model reveal that intraparticle diffusion is involved in the adsorption mechanism of MnO_4^- ions on investigated adsorbents and is not the limiting step and the only process controlling MnO_4^- ions adsorption. In contrast to AC-400, on the AC-600 adsorbent we obtain a slope with a coefficient of linear regression close to 1. This result reveals that intraparticle diffusion on the AC-600 bed plays an important role in the adsorption mechanism of MnO_4^- ions.

Based on these results, the prepared activated carbon can be used in fixed bed dynamic adsorption processes for the removal of MnO_4^- ions from acidic aqueous solution, in particular the AC-400 adsorbent whose bed shows a better efficiency.

Acknowledgments

The authors are grateful to Professor Samuel Mignard and the CNRS Research Fellow of IC2MP for their help in the characterization of materials.

Conflicts of Interest

The authors declare no conflicts of interest regarding the publication of this paper.

References

[1] Les communautés confrontées aux engagements de déforestation zéro (2020) Le cas d'OLAM au Gabon, Muyissi Environnement et Mouvement Mondial pour les Forêts Tropicales (WRM).

[2] Sethupathi, S., Bashir, M.J.K., Ali Akbar, Z. and Mohamed, A.R. (2015) Biomass-Based Palm Shell Activated Carbon and Palm Shell Carbon Molecular Sieve as Gas Separation Adsorbents. *Waste Management & Research*: *The Journal for a Sustainable Circular Economy*, **33**, 303-312. https://doi.org/10.1177/0734242X15576026

[3] Guo, J. and Lua, A.C. (2002) Characterization of Adsorbent Prepared from Oil-Palm Shell by CO_2 Activation for Removal of Gaseous Pollutants. *Materials Letters*, **55**, 334-339. https://doi.org/10.1016/S0167-577X(02)00388-9

[4] Kra, D.O., Atheba, G.P., Kouadio, N.A., Drogui, P. and Trokourey, A. (2021) Activated Carbon Based on Acacia Wood (*Auriculeaformis* , Côte d'Ivoire) and Application to the Environment through the Elimination of Pb^{2+} Ions in Industrial Effluents. *Journal of Encapsulation and Adsorption Sciences*, **11**, 18-43. https://doi.org/10.4236/jeas.2021.111002

[5] Brice, D.N.C., Manga, N.H., Arnold, B.S., Daouda, K., Victoire, A.A., Giresse, N.N.A., Nangah, C.R. and Nsami, N.J. (2021) Adsorption of Tartrazine onto Activated Carbon Based Cola Nuts Shells: Equilibrium, Kinetics, and Thermodynamics Studies. *Open Journal of Inorganic Chemistry*, **11**, 1-19. https://doi.org/10.4236/ojic.2021.111001

[6] Weidner, E. and Ciesielczyk, F.J.M. (2019) Removal of Hazardous Oxyanions from the Environment Using Metal-Oxide-Based Materials. *Materials*, **12**, Article 927. https://doi.org/10.3390/ma12060927

[7] Yang, J.B., Yu, M.Q. and Chen, W.T. (2015) Adsorption of Hexavalent Chromium from Aqueous Solution by Activated Carbon Prepared from Longan Seed: Kinetics, Equilibrium and Thermodynamics. *Journal of Industrial and Engineering Chemistry*, **21**, 414-422. https://doi.org/10.1016/j.jiec.2014.02.054

[8] Messi Me Ndong, A.N., Bouraima, A., Bissielou, C., Anguile, J.J. and Makani, T. (2021) Chemical Composition Assessment by Wavelength Dispersive X-Ray Fluorescence of Agricultural Soils in the Mining Town of Moanda, Gabon. *Journal of Agricultural Chemistry and Environment*, **10**, 345-358. https://doi.org/10.4236/jacen.2021.103022

[9] Oladoja, N.A. and Unouabonah, E.L. (2021) Progress and Prospect in the Management of Oxyanions Polluted Aqua Systems. In: Oladoja, N.A. and Unuabonah, E.I., Eds., *Environmental Contamination Remediation and Management*, Springer, berlin, 1-30. https://doi.org/10.1007/978-3-030-70757-6

[10] Mbaye, G. (2009) Synthèse et étude des charbons actifs pour le traitement des eaux usées d'une tannerie. Mémoire de Master, Institut Internationale d'Energie de l'Eau et de l'Environnement de Ouagadougou, Ouagadougou.

[11] Water (2012) Edition of the Drinking Water Standards and Health Advisories.

[12] Al-Aoh, H.A. (2019) Equilibrium, Thermodynamic and Kinetic Study for Potassium Permanganate Adsorption by Neem Leaves Powder. *Desalination and Water*

Treatment, **170**, 101-110. https://doi.org/10.5004/dwt.2019.24905

[13] Mve Mfoumou, C., Tonda-Mikiela, P., Ngoye, F., Mbouiti Berthy, L., Bouassa Mougnala, S., Sachse, A., Mignard, S. and Feuya Tchouya, G.R. (2022) Dynamic Adsorption on Fixed-Bed Column of Manganese Oxoanions (MnO_4^-) in Aqueous Media on Activated Carbon Prepared from Palm Nut Shells. *Journal of Environment Pollution and Human Health*, **10**, 58-70. https://doi.org/10.12691/jephh-10-2-4

[14] Bani-Atta, S.A. (2022) Potassium Permanganate Dye Removal from Synthetic Wastewater Using a Novel, Low-Cost Adsorbent, Modified from the Powder of *Foeniculum vulgare* Seeds. *Scientific Reports*, **12**, Article No. 4547. https://doi.org/10.1038/s41598-022-08543-z

[15] Amola, L.A., Kamgaing, T., Tchuifon, D.R.T., Atemkeng, C.D. and Anagho, S.G. (2020) Activated Carbons Based on Shea Nut Shells (*Vitellaria paradoxa*): Optimization of Preparation by Chemical Means Using Response Surface Methodology and Physicochemical Characterization. *Journal of Materials Science and Chemical Engineering*, **8**, 53-72. https://doi.org/10.4236/msce.2020.88006

[16] Belin, T., Mve Mfoumou, C., Mignard, S. and Pouilloux, Y. (2013) Study of Physisorbed Carbon Dioxide on Zeolites Modified by Addition of Oxides or Acetate Impregnation. *Microporous and Mesoporous Materials*, **182**, 109-116. https://doi.org/10.1016/j.micromeso.2013.08.020

[17] Brunauer, S., Emmett, P.H. and Teller, E. (1938) Adsorption of Gases in Multimolecular Layers. *Journal of the American Chemical Society*, **60**, 309-319. https://doi.org/10.1021/ja01269a023

[18] Lippens, B.C. and de Boer, J.H. (1965) Studies on Pore Systems in Catalysts: V. the *t* Method. *Journal of Catalysis*, **4**, 319-323. https://doi.org/10.1016/0021-9517(65)90307-6

[19] Lynch, J., Raatz, F. and Dufresne, P. (1987) Characterization of the Textural Properties of Dealuminated HY Forms. *Zeolites*, **7**, 333-340. https://doi.org/10.1016/0144-2449(87)90036-4

[20] de Boer, J.H., Lippens, B.C., Lisen, B.G., Broekhoff, J.C.P., Van Den Heuvel, A. and Osinga, T.J. (1966) The*t*-Curve of Multimolecular N2-Adsorption. *Journal of Colloid and Interface Science*, **21**, 405-414. https://doi.org/10.1016/0095-8522(66)90006-7

[21] Boehm, H.P. (1966) Chemical Identification of Surface Groups. *Advances in Catalysis*, **16**, 179-274. https://doi.org/10.1016/S0360-0564(08)60354-5

[22] Mve Mfoumou, C., Tonda-Mikiela, P., Ngoye, F., Belin, T. and Mignard, S. (2022) Dynamic Adsorption and Desorption of CO_2 from Binary Mixtures of CH_4 and C_3H_8 on X Type Zeolites. *American Journal of Environmental Protection*, **10**, 83-90.

[23] Mfoumou, C.M., Ngoye, F., Tonda-Mikiela, P., Evoung, F.E., Bi-Ndong, L.B., Belin, T. and Mignard, S. (2023) Study of the Temperature-Programmed Desorption of Carbon Dioxide (CO_2) on Zeolites X Modified with Bivalent Cations. *Journal of Environmental Protection*, **14**, 66-82. https://doi.org/10.4236/jep.2023.141005

[24] Zahra, S., Reyhane, S. and Reza, F. (2013) Fixed-Bed Adsorption Dynamics of Pb (II) Adsorption from Aqueous Solution Using Nanostructured γ-Alumina. *Journal of Nanostructure in Chemistry*, **3**, Article No. 48. https://doi.org/10.1186/2193-8865-3-48

[25] Goertzen, S.L., Thérault, K.D., Oickel, A.M., Tarasuk, A.C. and Andreas, H.A. (2010) Standardization of the Boehm Titration. Part I. CO_2 Expulsion and Endpoint Determination. *Carbon*, **48**, 1252-1261.

https://doi.org/10.1016/j.carbon.2009.11.050

[26] Lagergren, S. (1898) Zur Theorie der Sogenannten Adsorption Gelöster Stoffe, Kungliga Svenska Vetenskapsakademiens. *Handlingar*, **24**, 1-39.

[27] Blanchard, G., Maunaye, M. and Martin, G. (1984) Removal of Heavy Metals from Waters by Means of Natural Zeolites. *Water Research*, **18**, 1501-1507. https://doi.org/10.1016/0043-1354(84)90124-6

[28] HO, Y.S. and Mckay. G. (1999) Pseudo-Second Order Model for Sorption Processes. *Process Biochemistry*, **34**, 451-465. https://doi.org/10.1016/S0032-9592(98)00112-5

[29] Weber, J.W. (1972) Physicochemical Process for Water Quality Control (Metcalf, R.L. and Pitts, J.N., Eds.). Wiley International Science, New York, 199-259.

[30] Sing, K.S.W., Everett, D.H., Haul, R.A.W., Moscou, L., Pierotti, R.A., Rouquerol, J. and Siemieniewska, T. (1985) Reporting Physisorption Data for Gas/Solid Systems with Special Reference to the Determination of Surface Area and Porosity (Recommendations 1984). *Pure and Applied Chemistry*, **57**, 603-619. https://doi.org/10.1351/pac198557040603

[31] Malkoc, E. and Nuhoglu, Y. (2006) Removal of Ni (II) Ions from Aqueous Solutions Using Waste of Tea Factory: Adsorption on a Fixed-Bed Column. *Journal of Hazardous Materials*, **135**, 328-336. https://doi.org/10.1016/j.jhazmat.2005.11.070

[32] Tan, I., Ahmad, A. and Hameed, B.H. (2009) Fixed-Bed Adsorption Performance of Oil Palm Shell-Based Activated Carbon for Removal of 2, 4, 6-Trichlorophenol. *Bioresource Technology*, **100**, 1494-1496. https://doi.org/10.1016/j.biortech.2008.08.017

[33] Alamrani, N.A., Al-Aoh, H.A., Aljohani, M.M.H., Bani-Atta, S.A., Sobhi, M., Khalid, M.S., Darwish, A.A.A., Keshk, A.A. and Abdelfattah, M.A.A. (2021) Wastewater Purification from Permanganate Ions by Sorption on the *Ocimum basilicum* Leaves Powder Modified by Zinc Chloride. *Journal of Chemistry*, **2021**, Article ID: 5561829. https://doi.org/10.1155/2021/5561829

[34] Mahmoodi, N.M., Hayati, B., Arami, M. and Lan, C. (2011) Adsorption of Textile Dyes on Pine Cone from Colored Wastewater: Kinetic, Equilibrium and Thermodynamic Studies. *Desalination*, **268**, 117-125. https://doi.org/10.1016/j.desal.2010.10.007